Angewandte Chemie
Eine Zeitschrift der Gesellschaft Deutscher Chemiker

Supporting Information

Tunable Syngas Production from CO_2 and H_2O in an Aqueous Photoelectrochemical Cell

*Sheng Chu, Shizhao Fan, Yongjie Wang, David Rossouw, Yichen Wang, Gianluigi A. Botton, and Zetian Mi**

ange_201606424_sm_miscellaneous_information.pdf

Supporting Information

Experimental Section

Synthesis:

All chemicals were obtained from commercial suppliers and used without further purification. GaN nanowire arrays were grown on p-n junction Si wafer by plasma-assisted molecular beam epitaxy (MBE) under nitrogen-rich conditions according to our previous work.[1] The p-n junction Si wafer was fabricated using a standard thermal diffusion process. The MBE growth conditions included a growth temperature of 750 ^{o}C for 1 h, a nitrogen flow rate of 1.0 standard cubic centimeter per minute (sccm), a forward plasma power of 350 W, and Ga flux ~ 8×10^{-8} Torr.

Cu and ZnO were photodeposited on GaN/n^{+}-p Si via a simple solution-based process. The photodeposition process was performed in a sealed Pyrex chamber with a quartz lid. First, the GaN/n^{+}-p Si wafer sample was fixed in a Teflon holder and placed in the chamber. Then, 60 mL deionized water (purged with Ar for 20 min before use), 2 mL of 0.2 M $Zn(NO_3)_2$ (98%, Sigma Aldrich), 20 μL of 0.2 M $Cu(NO_3)_2$ (99%, Sigma Aldrich), and 15 mL methanol (99.8%, ACP Chemicals) as the sacrificial electron donor were added in sequence. The reaction chamber was then evacuated and irradiated for 30 min using 300 W Xenon lamp (Excelitas Technologies) for the photodeposition of Cu and ZnO. ZnO were deposited via $Zn(OH)_2$ intermediate through the reaction between zinc ions (Zn^{2+}) and hydroxide ions (OH^{-}).[2] The source of OH^{-} came from the reduction of nitrate ions (NO_3^{-}) and H_2O by photogenerated electrons from GaN nanowires.[3] For the deposition of Cu, it was synthesized directly from the reduction of Cu^{2+} by energetic photogenerated electrons due to the rather positive redox potential of Cu^{2+}/Cu (+0.342 V versus NHE at pH 0).[4] Finally, the as-prepared sample was heated at a rate of 20 ^{o}C/min to reach 300 ^{o}C and maintained for 2 h under an Ar flow

rate of 100 sccm. Then the sample was naturally cooled down to room temperature in a flowing-argon atmosphere.

For comparison, Cu/GaN/n^+-p Si was prepared using the same protocol except for the absence of $Zn(NO_3)_2$. And Au-ZnO/GaN/n^+-p Si, Ag-ZnO/GaN/n^+-p Si were prepared by following the same protocol except for the use of $HAuCl_4$ (99.9%, Sigma Aldrich) and $AgNO_3$ (99%, Sigma Aldrich) instead of $Cu(NO_3)_2$.

Characterization:

SEM image was taken using an Inspect F-50 FE-SEM system. TEM image was acquired on FEI Tecnai G2 F20 microscope operated at 200 kV. The nanowires were scratched off from the substrate onto a TEM grid. XRD pattern was collected on a Bruker D8 Discovery X-ray diffractometer using Cu Kα source. XPS was performed in a Thermo Scientific K-Alpha XPS system with a monochromatic Al Kα source (hv=1486.6 eV). Charging effects were compensated by applying a flood gun, and binding energies were calibrated with respect to the C 1s level 284.8 eV of contaminated carbon.

The CO_2 adsorption capability of the samples was evaluated via a modified route according to the reported procedure.[5] The sample was first degassed at 300 ^oC for 1 h under evacuation and then cooled to room temperature, followed by introduction of high-purity CO_2 (Air Liquid, 99.995%) into the system to reach 1 atm for 0.5 h to reach equilibrium. Then the system was flushed with Ar (Air Liquid, 99.999%) for 1 h to remove any CO_2 not adsorbed or weakly adsorbed, which was checked by gas chromatograph (GC, Shimadzu GC-2014). Afterwards, the sample was heated to desorb CO_2, which was detected and quantified by the GC.

Photoelectrochemical measurements:

The photoelectrochemical experiments were performed in a conventional three-electrode cell, which consists of Cu-ZnO/GaN/n^+-p Si as the working

electrode (WE), a Pt wire as the counter electrode (CE), and Ag/AgCl (saturated KCl) as the reference electrode (RE). The electrolyte (40 mL) was CO_2-saturated aqueous solution of 0.5 M $KHCO_3$ (Fisher Chemical) with a pH of ~8. The working electrode (~0.2 cm^2) was prepared as follows: an alloy of Ga-In eutectic (99.99%, Sigma-Aldrich) was put on the backside of the Si substrate, which was subsequently attached to a copper wire with the aid of silver paint (Ted Pella). Then, epoxy (PC-Clear) was used to insulate and protect the back contact between Si and copper wire. Prior to every measurement, the working electrode compartment was purged with CO_2 for 30 min. A 300 W Xenon lamp (Excelitas Technologies) was used as the light source. The light intensity on the sample is about 800 mW cm^{-2} (~8 suns). The current and potential data were collected by an Interface 1000 potentiostat (Gamry Instruments). The scan rate of current-potential (J-V) curve is 20 mV/s. After the photoelectrolysis, a small fraction of headspace products in the working compartment (40 mL) was sampled by gas-tight syringe and analyzed by a thermal conductivity detector (for H_2) and a flame ionization detector (for CO and hydrocarbons) of GC. Liquid products of electrolyte were analyzed afterwards by quantitative NMR (Bruker AV-500) using 4,4-dimethyl-4-silapentane-1-sulfonic acid (DSS, Sigma Aldrich) as an internal standard. Faradaic efficiency (FE) was calculated from the amount of charge passed to form each product divided by the total charge passed. Repeated measurement was conducted to check the consistency of the experiments.

In ^{13}C-labeled isotope experiment, the working electrode was immersed in ^{13}C-bicarbonate solution ($NaH^{13}CO_3$, 98%, Sigma Aldrich) through which $^{13}CO_2$ (99%, Sigma Aldrich) was purged for 30 min. Photoelectrolysis was conducted at −0.23 V vs. RHE for 100 min. The gas products were detected by gas chromatography mass spectrum (GC-MS, Agilent 5975).

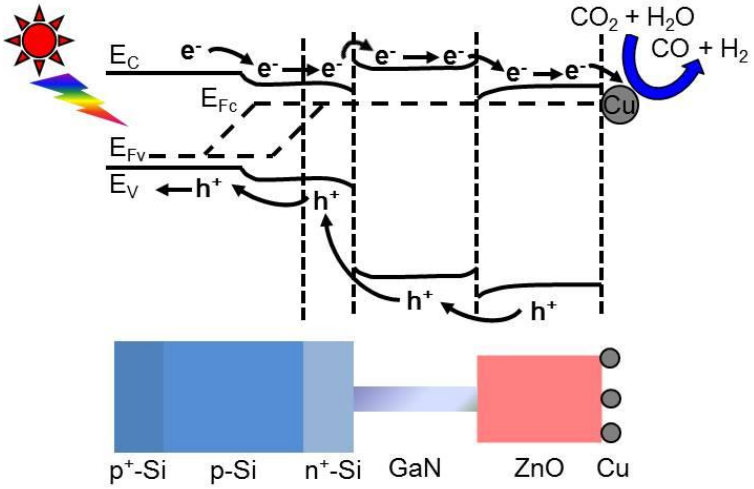

Figure S1. Energy band diagram of Cu-ZnO/GaN/n^+-p Si under illumination. The electron affinity of n-Si is reported to be about 4.05 eV.[6] The electron affinity of n-GaN is reported to be in the range of 3.5 eV to 4.1 eV.[7] And it is reported that the n-GaN/n-Si heterointerface has a very small energy barrier for electron transport.[8] In this study, both Si and GaN are heavily n-type doped, which can facilitate the electron transfer from Si to GaN. Furthermore, under light illumination, the abundance of photogenerated electrons leads to flat-band condition, which reduces the upward bending of surface energy and facilitates the electron injection from n^+-Si layer to n-GaN at a small applied bias. The electron affinity of ZnO is reported to be in the range of 4.2 eV to 4.6 eV.[9] The higher electron affinity of ZnO compared to GaN facilitate the electron transfer from GaN to ZnO via the intimate interface due to the close lattice match between them.

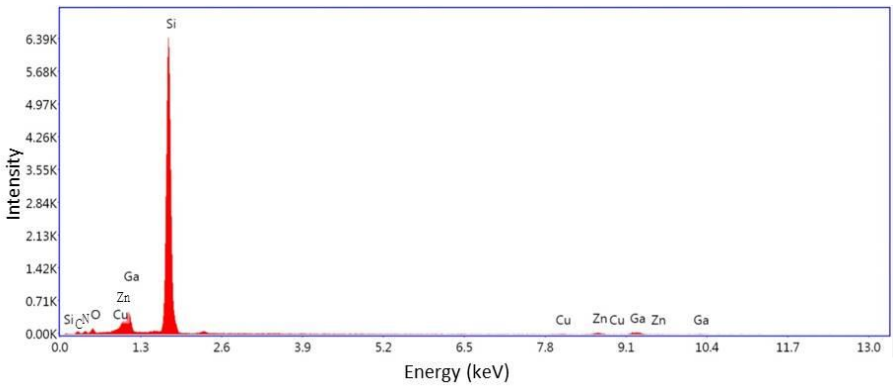

Figure S2. EDX spectrum of Cu-ZnO/GaN/n^+-p Si. The Cu/Zn atomic ratio is about 1 : 6 from the EDX analysis.

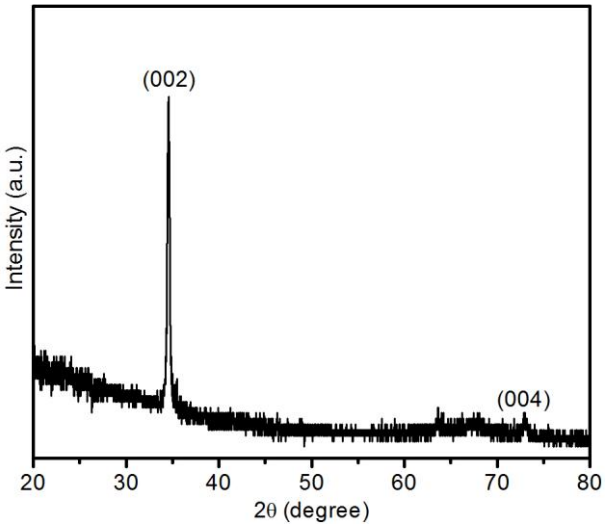

Figure S3. XRD pattern of Cu-ZnO/GaN/n^+-p Si. The (002) and (004) peaks from GaN confirm the preferential nanowire growth along the c-axis <0001> direction. The absence of XRD peaks of Cu and ZnO is probably due to their low contents and small nanoscale crystalline sizes.

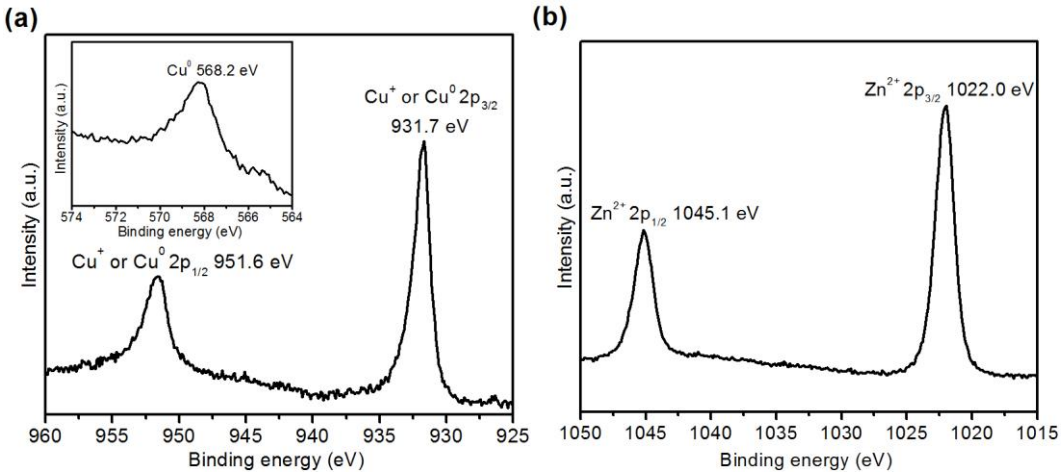

Figure S4. XPS of (a) Cu 2p and (b) Zn 2p for Cu-ZnO/GaN/n^+-p Si. Inset: Cu LMM Auger spectrum. The binding energy of 931.7 and 951.6 eV can be assigned to either Cu^+ or Cu^0.[10] The presence of Cu^{2+} species is ruled out based on the absence of a characteristic peak around 933.5 eV and the shake-up satellite peak at ~942.5 eV.[10] The difference between Cu^+ and Cu^0 species can be identified by the Auger Cu LMM transition, where Cu^+ peak appears by ~2 eV higher than Cu^0 peak in the term of binding energy.[11] The single Auger peak at 568.2 eV indicates the presence of only metallic Cu (Cu^0). The binding energy of 1022.0 and 1045.1 eV are typical Zn 2p XPS spectra associated with Zn^{2+}.[12]

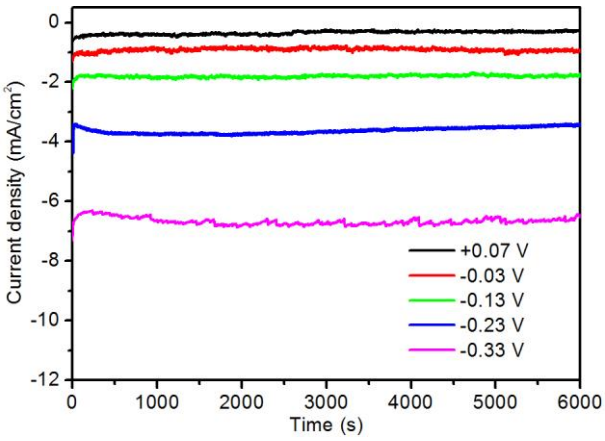

Figure S5. Chronoamperometry data at different applied potentials in CO_2-saturated aqueous solution of 0.5 M $KHCO_3$ (pH 8).

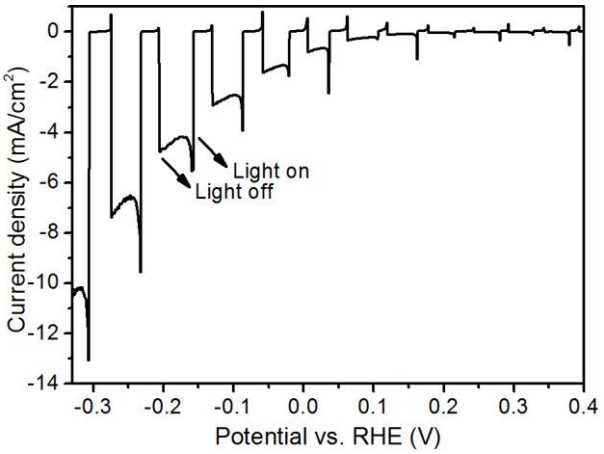

Figure S6. J-V curve of Cu-ZnO/GaN/n^+-p Si photocathode under chopped illumination. No photocurrent was observed when the illumination on the photocathode was blocked.

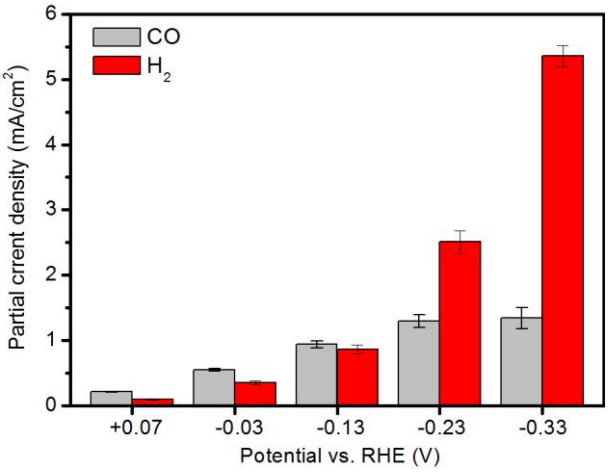

Figure S7. Partial current density for CO (grey bars) and H_2 (red bars) of Cu-ZnO/GaN/n^+-p Si photocathode as a function of potential.

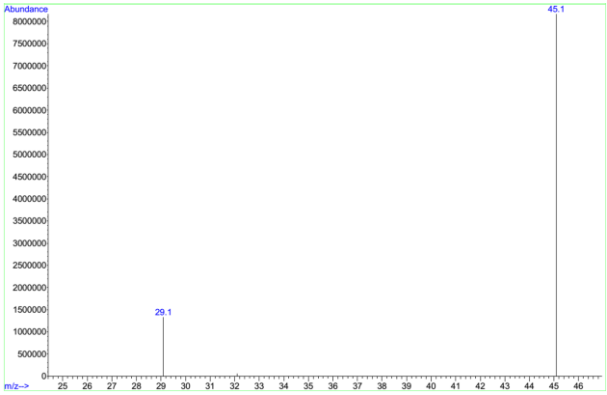

Figure S8. MS chromatogram of the gas phase analysis after ^{13}C-labeled isotope experiment.

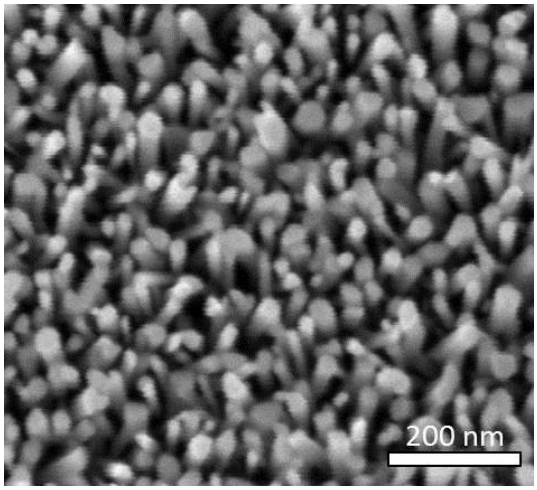

Figure S9. A top view SEM image of GaN nanowires grown on a p-n junction Si. Because the direct calculation of Cu and ZnO loading amount from SEM image is difficult, we calculated them based on the well-defined GaN nanowire arrays and the ratio of (Cu+Zn) : Ga by EDX analysis. From the top view SEM image of GaN nanowire arrays, the estimated fill factor of GaN nanowire on Si substrate is about 40%. Considering the length of nanowires is ~150 nm, the used sample area is 0.2 cm^2, and the density of GaN is 6.1 g/cm^3, the amount of GaN nanowires is calculated to be 7.32 μg (~0.087 μmol). Then the total amount of Cu and ZnO corresponds to ~0.05 μmol based on the (Cu+Zn) : Ga ratio of (0.17+1.05) : 2.15 by EDX analysis.

The turnover number reported in this work (1330) is greatly underestimated because the calculation is based on the bulk Cu-ZnO catalyst instead of only the surface active sites. By considering only the surface sites, the turnover number is calculated as below:[13]

First, the specific surface areas of Cu nanoparticles (S_{Cu}) and ZnO nanosheets (S_{ZnO}) are calculated. Considering the average size of Cu nanoparticles is ~7 nm, S_{Cu} is calculated to be ~96 m^2/g from the formula of 6/(d*D), where d is the density of Cu (8.9 g/cm^3) and D is the diameter of Cu nanoparticle (7 nm). Considering the average size of ZnO nanosheets is 400 nm and thicknesses is about 10 nm, S_{ZnO} is calculated to be ~37 m^2/g from the formula of 2 * (L*W + W*H + H*L), Where L, W and H are the length, width and height of ZnO nanosheet, respectively.

Second, the loading amount of Cu nanoparticles (M_{Cu}) and ZnO nanosheets (M_{ZnO}) are calculated to be 0.44 μg and 3.63 μg, respectively. This is based on the Cu : Ga and Zn : Ga atomic ratios are 0.17 : 2.15 and 1.05 : 2.15 respectively by EDX analysis, and the amount of GaN nanowires has been calculated to be ~0.087 μmol (see the supporting information).

Third, the area of single Cu atom ($S_{Cu\ atom}$) and Zn atom ($S_{Zn\ atom}$) are calculated to be 0.21 nm^2 and 0.23 nm^2, respectively. This is estimated by considering the atoms are spheres and the atomic radii of Cu and Zn are 0.128 nm and 0.134 nm, respectively.

Finally, the molar amount of surface Cu and Zn are calculated to be 0.33 nmol and 0.97 nmol respectively, from the formula of $(S_{Cu} * M_{Cu})/(S_{Cu\ atom} * N_v)$, where N_v is the Avogadro's number (6.02×10^{23} mol^{-1}). Therefore, the TON, calculated from the ratio of the total amount of gas evolved (66.5 μmol) and the total surface sites (1.3 nmol), is estimated to be ~51150. It is worth noting that such a value is a lower limit since it assumes all surface sites are active sites. However, the estimation of the number of active sites is difficult because the complexity of heterogeneous photocatalysis (e.g. defects may be the active sites, the uncertainty of the irradiated area of the photocatalyst surface).[14]

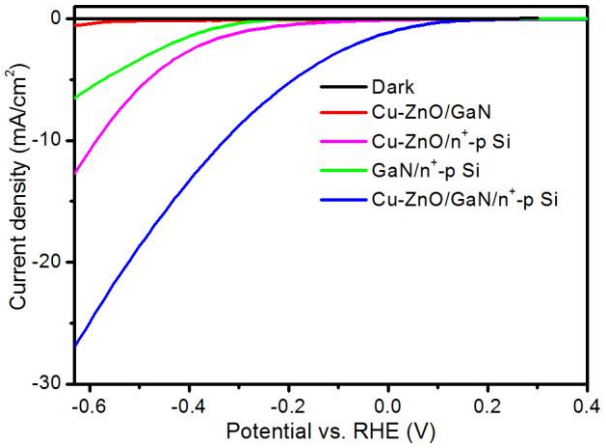

Figure S10. J-V curves of different photocathodes.

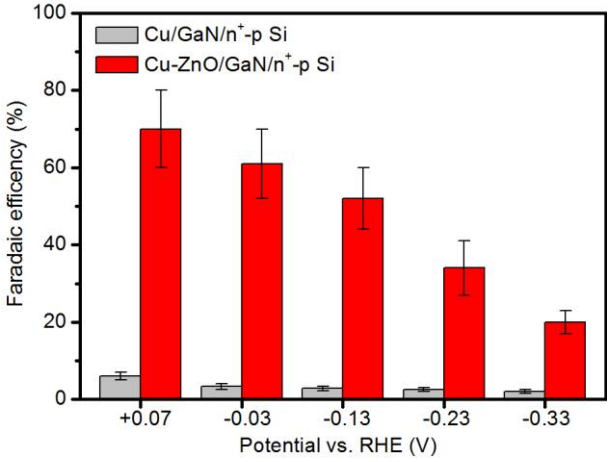

Figure S11. FEs for CO of Cu/GaN/n$^+$-p Si and Cu-ZnO/GaN/n$^+$-p Si at different potentials.

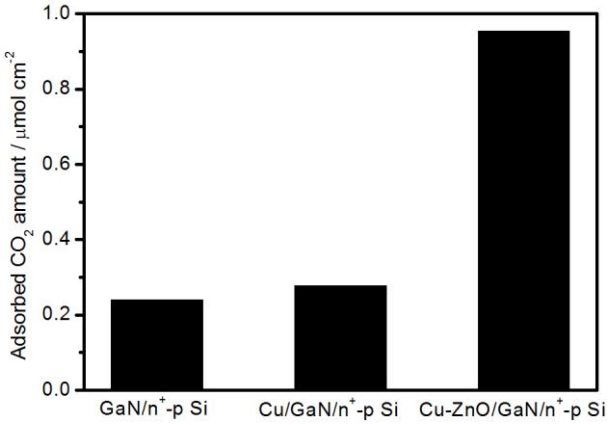

Figure S12. CO_2 adsorption capacity of different samples.

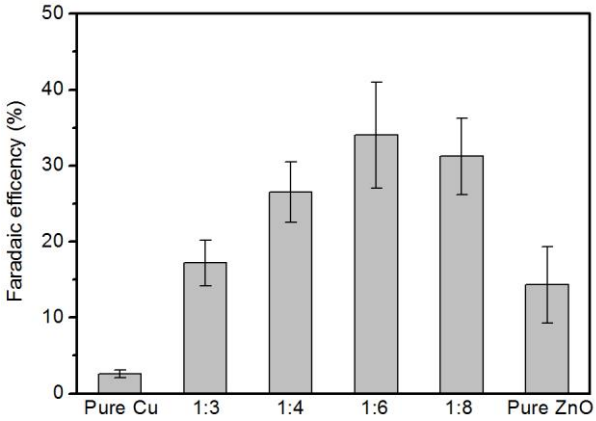

Figure S13. FEs for CO of different Cu/Zn ratios at −0.23 V vs. RHE. The Cu/Zn atomic ratios were estimated from the EDX analysis. The data of pure ZnO was obtained at −0.33 V vs. RHE. In the low ZnO content region, it was found that the Faradaic efficiency for CO increased obviously after the increasing of ZnO amount, indication the important role of ZnO in enhancing the selectivity for CO_2 reduction to CO. The maximum Faradaic efficiency for CO was obtained at a Cu/Zn ratio of 1:6. Further increasing the loading of ZnO does not improve the CO selectivity, probably due to the proton-coupled electron transfer on Cu rather than the adsorption of CO_2 on ZnO becomes the rate-determining step for the CO formation reaction. Therefore, there is a balance of CO_2 adsorption on ZnO and proton-coupled electron transfer on Cu to achieve the highest formation rate of CO.

Due to the synergetic co-catalytic effect of Cu and ZnO on CO_2 reduction to CO, CO can be formed at relatively high rate at low applied bias. At high applied bias, CO_2 adsorption on ZnO becomes the rate-determining step for the CO formation due to the mass transfer limitation of CO_2 to the electrode surface. Improvements in mass transport by applying a gas diffusion electrode are expected to enable a high rate of CO_2 reduction at high bias operation.[15]

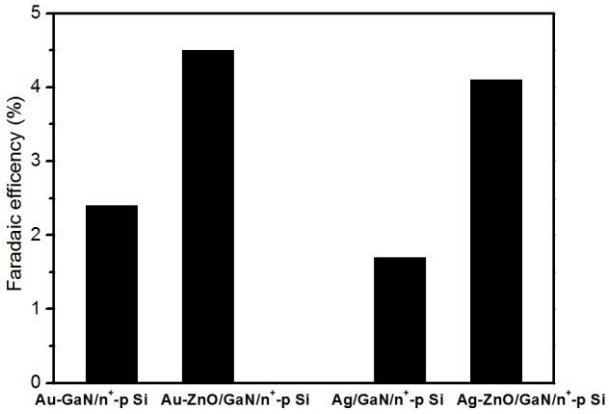

Figure S14. FEs for CO of different photocathodes at −0.23 V vs. RHE.

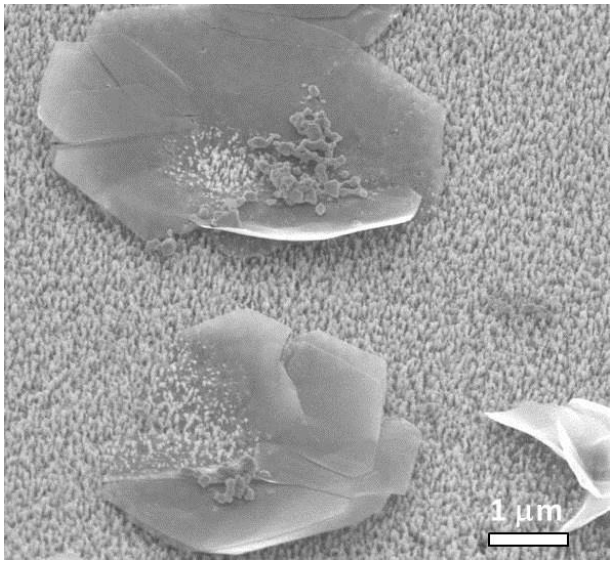

Figure S15. SEM image of Au-ZnO/GaN/n^+-p Si sample.

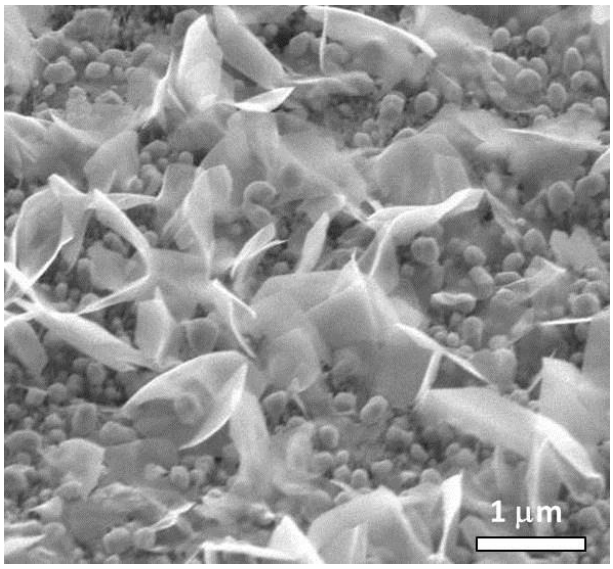

Figure S16. SEM image of Ag-ZnO/GaN/n^+-p Si sample.

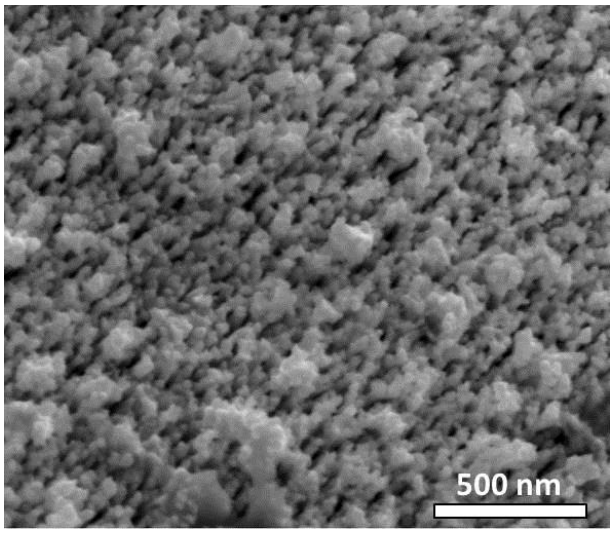

Figure S17. SEM image of Cu/GaN/n^+-p Si sample.

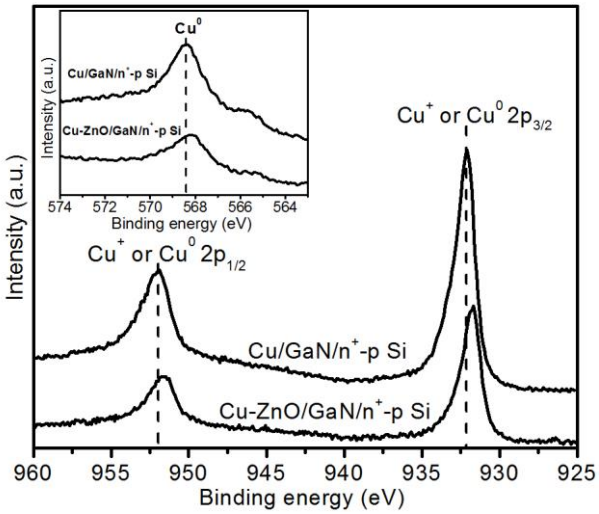

Figure S18. XPS of Cu 2p of Cu/GaN/n^+-p Si and Cu-ZnO/GaN/n^+-p Si. Inset: Cu LMM Auger spectrum.

Reference:

[1] a) S. Fan, B. AlOtaibi, S. Y. Woo, Y. Wang, G. A. Botton, Z. Mi, *Nano Lett.* **2015**, *15*, 2721-2726; b) Y. Wang, S. Fan, B. AlOtaibi, Y. Wang, L. Li, Z. Mi, *Chem. Eur. J.* **2016**, *22*, 8809-8813.

[2] a) K. Uno, Y. Tauchi, I. Tanaka, *Jpn. J. Appl. Phys.* **2013**, *52*, 08JE16; b) J. J. Guan, H. Q. Wang, H. Liang, N. P. Cheng, H. Lin, Q. Li, Y. Li, L. Z. Qin, *RSC Adv.* **2015**, *5*, 52998-53002; c) T. Yoshida, D. Komatsu, N. Shimokawa, H. Minoura, *Thin Solid Films* **2004**, *451-452*, 166-169; d) X. Bai, L. Yi, D. Liu, E. Nie, C. Sun, H. Feng, J. Xu, Y. Jin, Z. Jiao, X. Sun, *Appl. Surf. Sci.* **2011**, *257*, 10317-10321.

[3] B. Bems, F. C. Jentoft, R. Schlogl, *Appl. Catal. B* **1999**, *20*, 155-163.

[4] P. Gomathisankar, K. Hachisuka, H. Katsumata, T. Suzuki, K. Funasaka, S. Kaneco, *Int. J. Hydrogen Energy* **2013**, *38*, 11840-11846.

[5] a) Y. Y. Li, K. K. Han, W. G. Lin, M. M. Wan, Y. Wang, J. H. Zhu, *J . Mater. Chem. A* **2013**, *1*, 12919-12925; b) F. Frusteri, M. Cordaro, C. Cannilla, G. Bonura, *Appl. Catal. B* **2015**, *162*, 57-65.

[6] S. M. Sze, K. K. Ng, *Physics of semiconductor devices*, *3rd Edition*, John Wiley & Sons, Hoboken, **2007**, 790.

[7] a) V. Bougrov, M.E. Levinshtein, S. L. Rumyantsev, A. Zubrilov, *Properties of Advanced SemiconductorMaterials GaN, AlN, InN, BN, SiC, SiGe*, John Wiley & Sons, New York, **2001**, 1-30. b) H. Morkoc, *Handbook of Nitride Semiconductors and Devices*, Wiley-VCH, Weinheim, **2008,** 18; c) C. Wu, A. Kahn, N. Taskar, D. Dorman, D. Gallagher, *J. Appl. Phys.* **1998**, *83*, 4249-4252.

[8] S. Guha, N. A. Bojarczuk, *Appl. Phys. Lett.* **1998**, *72*, 415-417.

[9] S. A. Chevtchenko, J. C. Moore, U. Ozgur, X. Gu, A. A. Baski, H. Morkoc, B. Nemeth, J. E. Nause, *Appl. Phys. Lett.* **2006**, *89*, 182111.

[10] L. Liu, F. Gao, H. Zhao, Y. Li, *Appl. Catal. B* **2013**, *134-135*, 349-358.

[11] T. Waechtler, S. Oswald, N. Roth, A. Jakob, H. Lang, R. Ecke, S. E. Schulz, T. Gessner, A. Moskvinova, S. Schulze, M. Hietschold, *J. Electrochem. Soc.* **2009**, *156*, H453-H459.

[12] Y. J. Jang, J.-W. Jang, J. Lee, J. H. Kim, H. Kumagai, J. Lee, T. Minegishi, J. Kubota, K. Domen, J. S. Lee, *Energy Environ. Sci.* **2015**, *8*, 3597-3604.

[13] a) F. Wang, C. Li, L.-D. Sun, H. Wu, T. Ming, J. Wang, J. C. Yu, C.-H. Yan*, J. Am. Chem. Soc.* **2011**, *133*, 1106-1111; b) X. C. Wang, K. Maeda, A. Thomas, K. Takanabe, G. Xin, J. M. Carlsson, K. Domen, M. Antonietti, *Nat. Mater.* 2009, **8,** 76-80.

[14] a) M. Boudart, *Chem. Rev.* **1995**, *95*, 661-666; b) A. V. Emeline, A. V. Panasuk, N. Sheremetyeva, N. Serpone, *J. Phys. Chem. B*, **2005**, *109*, 2785-2792.

[15] C. Delacourt, P. L. Ridgway, J. B Kerr, J. Newman, *J. Electrochem. Soc.* **2008**, *155*, B42-B49.